










LETTER | OCTOBER 22 2024

# Isolator-free quantum dot comb lasers with optical feedback enhanced DWDM transmission

Xiangru Cui ; Jiajian Chen ; Jingzhi Huang; Bo Yang ; Jiale Qin ; Wenlu Wang ; Jianan Duan ; Ting Wang ; Zihao Wang  ; Jianjun Zhang



APL Photonics 9, 101305 (2024)

<https://doi.org/10.1063/5.0222404>



View  
Online



Export  
Citation

## Articles You May Be Interested In

S, C and L-band photonic DWDM system design and spectral analysis

*AIP Conf. Proc.* (October 2023)

Modulation techniques in DWDM systems: A comprehensive review of current challenges and future directions

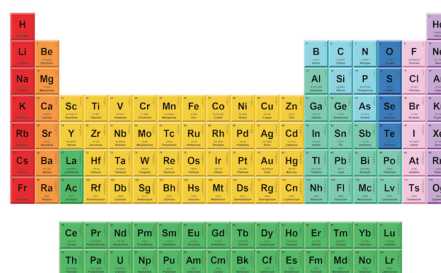
*AIP Conf. Proc.* (October 2024)

Analysis of Stimulated Raman Scattering on DWDM System

*AIP Conference Proceedings* (October 2011)



Now Invent.™



American Elements  
Opens a World of Possibilities

...Now Invent!

[www.americanelements.com](http://www.americanelements.com)

© 2021-2024 American Elements is a U.S. Registered Trademark

# Isolator-free quantum dot comb lasers with optical feedback enhanced DWDM transmission

Cite as: APL Photon. 9, 101305 (2024); doi: 10.1063/5.0222404

Submitted: 7 June 2024 • Accepted: 7 October 2024 •

Published Online: 22 October 2024



Xiangru Cui,<sup>1,2</sup> Jiajian Chen,<sup>3,4</sup> Jingzhi Huang,<sup>1,2</sup> Bo Yang,<sup>1,2</sup> Jiale Qin,<sup>1,2</sup> Wenlu Wang,<sup>5</sup> Jianan Duan,<sup>5</sup> Ting Wang,<sup>1,2,3,a)</sup> Zihao Wang,<sup>1,2,3,b)</sup> and Jianjun Zhang<sup>1,2,3</sup>

## AFFILIATIONS

<sup>1</sup> Beijing National Laboratory for Condensed Matter Physics, Institute of Physics, Chinese Academy of Sciences, Beijing 100190, China

<sup>2</sup> Center of Materials Science and Optoelectronic Engineering, University of Chinese Academy of Science, Beijing 100049, China

<sup>3</sup> Songshan Lake Materials Laboratory, Dongguan, Guangdong 523808, China

<sup>4</sup> The Department of Electrical and Electronic Engineering, The Hong Kong Polytechnic University, Kowloon, Hong Kong, China

<sup>5</sup> National Key Laboratory of Laser Spatial Information, School of Integrated Circuits, Harbin Institute of Technology, Shenzhen 518055, China

<sup>a)</sup> wangting@iphy.ac.cn

<sup>b)</sup> Author to whom correspondence should be addressed: wangzihao@iphy.ac.cn

## ABSTRACT

Feedback-insensitive Quantum Dot (QD) comb lasers hold significant promise for integrated dense wavelength division multiplexing photonic systems due to their ability to generate multiple wavelengths and operate without bulky isolators, facilitating the development of high-density and large-scale photonic integrated circuits. In this study, we investigated the optical feedback (OFB) influence of the InAs/GaAs QD comb laser from various perspectives. Our findings reveal that the comb laser exhibits a stable locking region with consistent optical spectra across a range of OFB strengths (−45 to −10 dB). Furthermore, under a high OFB strength of −10 dB, there is a notable 40 dB suppression of relative intensity noise in the low-frequency range (below 1 GHz). Transmission experiments demonstrate clear eye openings at 25 Gbps using a bit pattern of  $2^{31}-1$  pseudorandom binary sequence. Remarkably, the bit error rates decrease by five orders of magnitude under −10 dB OFB. These results indicate the ultra-robustness of 100 GHz grid QD comb laser, which exhibits great transmission enhancement under a strong OFB of −10 dB.

© 2024 Author(s). All article content, except where otherwise noted, is licensed under a Creative Commons Attribution (CC BY) license (<https://creativecommons.org/licenses/by/4.0/>). <https://doi.org/10.1063/5.0222404>

## I. INTRODUCTION

Semiconductor colliding pulse mode-locked (CPML) lasers as compact and low power consumption comb laser sources can generate high repetition rate pulses, which leads to broad application prospects in microwave photonics, arbitrary waveform generation, and high bandwidth dense wavelength division multiplexing (DWDM) transmission systems. In particular, for DWDM applications, CPML can be used as a multi-wavelength light source together with silicon photonic integrated circuits (PICs) to build

up high bandwidth and low power consumption optical I/O for high-performance computers and data centers.<sup>1</sup> However, optical feedback (OFB) inevitably occurs within DWDM systems either from the device packaging interfaces or from the reflections from the optical fiber links. These OFBs may deteriorate the laser stability and performance in terms of optical spectrum,<sup>2</sup> relative intensity noise (RIN),<sup>3</sup> bit error rate (BER) of external modulation,<sup>4</sup> etc. The increased BER caused by OFB can significantly degrade the data transmission performance. Optical isolators are commonly utilized

to eliminate the OFB impacts by using Faraday effects to block the reflected light re-entering the laser cavity. However, the bulky optical isolator brings up higher bills of material (BOM) costs and larger packaging footprints, limiting the compactness and scalability of PICs. Therefore, a comb laser with high OFB tolerance is crucial for integrated DWDM systems.

Due to the three-dimensional quantum confinement and the  $\delta$ -functional density of electron states of quantum dot (QD) structures, QD lasers exhibit several advantageous properties, including high-temperature stability,<sup>5</sup> low threshold current densities and high  $T_0$ ,<sup>6–8</sup> ultrafast carrier dynamics,<sup>5,9,10</sup> high differential gain,<sup>11,12</sup> small linewidth enhancement factor ( $\alpha$  factor),<sup>13,14</sup> and high damping rate.<sup>15</sup> The last three factors contribute to the OFB tolerance performance of QD lasers.<sup>16–20</sup> Previous studies have demonstrated feedback-insensitive InAs/GaAs QD Fabry–Perot (FP) lasers with near-zero  $\alpha$  factors, achieving penalty-free transmission rates of 10 Gbps under  $-7.4$  dB OFB through external modulation.<sup>21</sup> In addition, the ultrafast carrier characteristics and inhomogeneous gain spectrum broadening of QD enable the stable passively mode-locked and broad optical bandwidth comb laser, serving as an ideal multi-wavelength light source for DWDM applications. O-band passively mode-locked lasers with a repetition rate of 5–80 GHz have been achieved in previous studies.<sup>22–25</sup> However, studies on OFB tolerance have predominantly focused on two-section mode-locked laser designs with repetition frequencies typically up to 40 GHz.<sup>15,26–32</sup> These low repetition frequencies limit the maximum channel spacing, which can also result in severe crosstalk among adjacent channels at a high modulation rate in DWDM transmission systems.<sup>33</sup> Recently, we demonstrated QD comb lasers using a fourth-order CPML design, with a comb spacing of  $\sim 100$  GHz, matching the requirements of continuous-wave (CW)-WDM multi-source agree-

ments.<sup>34</sup> Moreover, the longer cavity of high-order CPML design preserves a large gain area, ensuring sufficient output power.<sup>20</sup> However, there is a lack of research on the effects of OFB on such CPML. Therefore, studying the OFB effects on high-order QD comb lasers is significant in evaluating their feedback tolerances for DWDM applications.

In this work, we present experimental findings on the OFB tolerance and transmission enhancement of an O-band 100 GHz InAs/GaAs QD comb laser featuring a fourth-order CPML design. We investigate the optical spectrum, RIN, and transmission performance of the laser under varied OFB strengths. Our results show that the locking conditions of the QD comb laser remain stable with OFB strength below  $-10$  dB. Under a flat-top optical spectral condition, eight comb lines within 3 dB optical bandwidth are achieved. Notably, both the wavelength and intensity of these comb lines remain stable across different OFB strengths. Analysis of the RIN for the eight filtered combs reveals suppression of low-frequency mode partition noise (MPN) under  $-10$  dB OFB, with an average RIN level of  $-130$  dBc/Hz. Furthermore, we conduct 25 Gbps non-return-to-zero (NRZ) modulations with each channel implementing a  $2^{31}-1$  pseudorandom binary sequence (PRBS31) pattern. The experimental results presented in this work show clear eye-diagrams and a significant BER reduction by five orders of magnitude, indicating that our QD comb laser with eight channels can achieve a total data transmission rate of 200 Gbps even under a strong OFB strength of  $-10$  dB.

## II. DEVICE AND EXPERIMENTAL ARRANGEMENT

In this work, the QD comb laser structure is grown via Molecular Beam Epitaxy (MBE) of InAs/GaAs QDs with an optimized

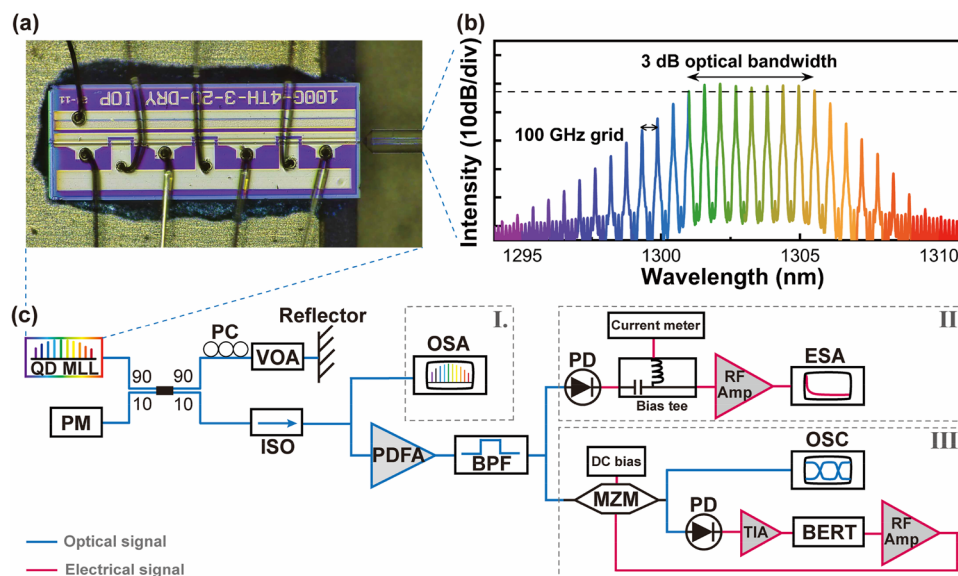


**FIG. 1.** (a) Micrograph of 100 GHz grid fourth order QD CPML. (b) Optical spectrum of 100 GHz grid fourth order QD CPML. (c) Experimental arrangement for the optical spectral (I), RIN (II), and transmission measurements (III) of QD 100 GHz mode-locked laser under different optical feedback strengths. VOA, variable optical attenuator; ISO, optical PM isolator; PDFA, praseodymium-doped fiber amplifier; BPF, bandpass filter; PC, polarization controller; MZM, Mach–Zehnder modulator; RF Amp: electrical amplifier; PD, photodetector; TIA, trans-impedance amplifier; PM, optical powermeter; OSA, optical spectrum analyzer; ESA, electrical spectrum analyzer; OSC, oscilloscope; and BERT, bit error rate tester.

seven-layer dot-in-a-well (DWELL) gain structure on an n-type GaAs(100) substrate.<sup>35–37</sup> The DWELL structure is implemented to decrease the leakage current and thus increases  $T_0$ .<sup>38</sup> The micrograph of the laser tested in this study with a fourth-order harmonic CPM structure is shown in Fig. 1(a). The total cavity length is 1580  $\mu\text{m}$ , corresponding to a fundamental repetition frequency of 25 GHz. Three saturable absorbers (SAs) are located at 1/4, 2/4, and 3/4 of the entire laser cavity, equally dividing it into four gain sections. By the dry etching of ridge waveguide to 100 nm above the active region, electrical isolation gaps are achieved. All the three SAs and four gain sections are electrically connected by wire bonding. The total length of three SAs is 10% of the entire cavity length, to avoid excessive power loss. In addition, the front facet is as-cleaved and the rear facet is deposited with high-reflection (HR) coating to boost the total output power. This laser structure allows four colliding pulses traveling intracavity to produce fourth-order harmonic pulses at 100 GHz repetition rate, while remains high output power compared with conventional two-section mode-locked lasers with a short gain cavity (1/4 cavity length of fourth-order CPML). Its typical optical spectrum is shown in Fig. 1(b). Multiple comb lines with 100 GHz comb spacing could be generated uniformly within a 3 dB optical bandwidth under certain mode-locked conditions. The detailed structural design and fabrication process of the device were described in our previous work.<sup>20</sup>

The under-tested QD comb laser is butterfly-packaged with the thermistor, thermoelectric cooler (TEC), and lensed fiber. The experimental setup is shown in Fig. 1(c), and the QD comb laser is driven in the continuous-wave (CW) mode by the current source (Keithley 2401), with three SAs reverse biased by a voltage source (Keysight E36102A), while the temperature is controlled at room temperature using a compact laser diode driver (Thorlabs CLD1015). A 10/90 fiber coupler is implemented to split the optical power, with 90% into a fiber based backreflector (BKR) for feedback tuning and 10% into an output port for further characterization. The BKR path consists of a polarization controller (PC), a variable attenuator (VOA) for continuous adjustment of OFB strength, and a polarization-maintaining BKR. By adjusting the voltage of VOA, the OFB strength can be tuned from  $-45$  to  $-10$  dB. The level of OFB strength is defined as the ratio of the optical power reflected back to the laser facet ( $P_{\text{reflected}}$ ) over the total output power of the laser

( $P_{\text{laser}}$ ) in decibel scale. The laser output power is collected by the lens fiber ( $P_{\text{out}}$ ), considering 3 dB coupling loss in the output direction but ignored in the reflection direction.  $P_{\text{reflected}}$  is obtained through the powermeter (PM) connected to the 10% port of the power splitter, as shown in Fig. 1(c). The power difference between 10% port ( $P_{10}$ ) and 90% port ( $P_{90}$ ) is calibrated to be 9.3 dB. As a result, the OFB strength (dB) =  $P_{\text{reflected}}$  (dBm)  $- P_{\text{laser}}$  (dBm) =  $(P_{10} + 9.3 \text{ dB}) - (P_{\text{out}} + 3 \text{ dB}) = P_{10} - P_{\text{out}} + 6.3 \text{ dB}$ . An optical isolator (ISO) is connected to the 10% output port, preventing unintentional OFB from the characterization side.

The optical spectrum is measured by the optical spectrum analyzer (OSA) (Yokogawa AQ6370D), as shown in section I of Fig. 1(c). To measure the RIN and high-speed optical transmission performance of QD comb laser under the influence of OFB, an O-band praseodymium-doped fiber amplifier (PDFA) (Thorlabs PDFA100) is used to compensate the relatively lower output power from 10% coupler port, and an O-band tunable bandpass filter (BPF) (EXFO XTM-50) is applied to filter out the single comb line for characterization. The RIN measurement setup [section II of Fig. 1(c)] consists of a photodetector (Optilab PD-40-M) with a responsivity of 0.640 A/W at 1300 nm, a bias tee connected with a current meter, a low-noise electrical amplifier (TLLA50K20G-30-30), and an electrical spectrum analyzer (ESA) (Keysight N9030B). The setup for the transmission performance measurement is shown in section III of Fig. 1(c). The filtered single comb line is coupled into a lithium niobate (LN) Mach-Zehnder modulator (MZM) (EOSPACE AX-0MVS-40) to modulate each comb channel externally. The 25 Gbps NRZ modulation signals are generated from a bit error rate tester (BERT) (Multilane ML4009) with a PRBS31 pattern. The electrical modulation signals are amplified through a 50 GHz bandwidth RF amplifier (Optilab MD50). The external modulated signals are sent to an optical sampling oscilloscope (Agilent DCA-X 86110D) to show the optical eye diagram. A 40 GHz bandwidth PIN receiver module (Optilab PD-40-M) is used to capture the optical modulated signals and generate RF signals for the BER measurement.

### III. RESULTS AND DISCUSSION

Figure 2 shows the continuous-wave light current (L-I) characteristics of the QD comb laser at different feedback strengths. The

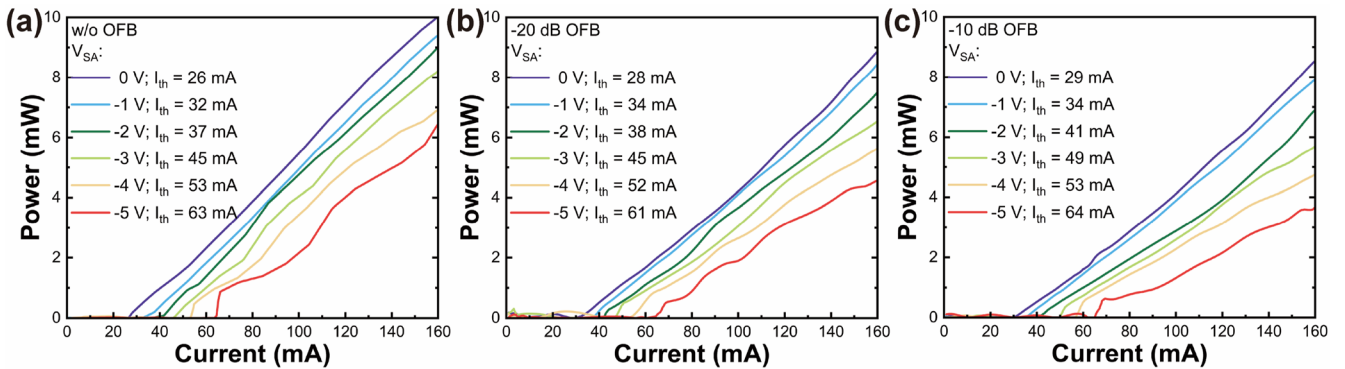


**FIG. 2.** Room temperature continuous-wave light current (L-I) characteristics of the QD 100 GHz comb laser measured in this work at varied reverse bias voltages from 0 to  $-5$  V, under different OFB strengths: (a) Without OFB, (b)  $-20$  dB OFB, and (c)  $-10$  dB OFB. The threshold current ( $I_{th}$ ) of each working condition is labeled in the legend.

optical power of butterfly-packaged comb lasers is collected by a lens fiber with  $\sim 3$  dB coupling loss. Consequently, the actual optical output power of the laser [ $P_{\text{laser}}$  (mW)] should be doubled the measured value [ $P_{\text{out}}$  (mW)] here. As the reverse bias voltage of SA ( $V_{\text{SA}}$ ) increases from 0 to 5 V, the threshold current ( $I_{\text{th}}$ ) increases, while the slope efficiency also degrades slightly, leading to the reduction in output power, as shown in Fig. 2(a). The increased  $V_{\text{SA}}$  leads to higher non-saturated losses within the SA section,<sup>20,27,39,40</sup> requiring higher injected current to lase. The abrupt kinks beyond  $I_{\text{th}}$  indicate the sudden cavity loss originated from the nonlinear saturation effect of the SA.<sup>41,42</sup> As shown in Figs. 2(b) and 2(c), the output power decreases with the increased OFB strength. This decrease is attributed to the coherence feedback mechanism<sup>43</sup> of in-phase pulse lasers. Under OFB, those modes near the in-phase condition have a lower threshold gain, while other photons suffer from higher cavity loss, leading to a decline in the output power.<sup>40</sup> In addition,  $I_{\text{th}}$  varies with different OFB strengths, possibly due to the balance between more feedback photons provided by external coherent light and increased intracavity losses induced by OFB coupling.

For high-capacity DWDM applications, the number of comb lines within 3 dB optical bandwidth of QD comb lasers [illustrated in Fig. 1(b)] is an essential figure of metrics that determines the maximum available transmission channels in DWDM systems. Thus, the optical spectral mappings of the comb laser under different operating conditions with varied OFB strengths were carried out. In order to reflect spectral flatness, if one or a few comb lines fall below

3 dB optical bandwidth, it is considered unlocked, corresponding to zero comb number. The  $V_{\text{SA}}$  was swept from 0 to  $-5$  V with 0.2 V step, and the injection current of gain sections ( $I_{\text{inj}}$ ) was swept from 40 to 160 mA with 2 mA step. Figure 3(a) shows 3 dB optical bandwidth mapping of the QD comb laser in terms of comb numbers without external OFB. Under low injection current conditions ( $I_{\text{inj}} = 40$ –100 mA), the stable mode-locked area is obtained by applying low  $V_{\text{SA}}$ . Because excessive  $V_{\text{SA}}$  introduces a much higher cavity loss, it is thus difficult to form a stable optical frequency comb. Under high injection current conditions ( $I_{\text{inj}} > 100$  mA), additional comb lines are obtained with a broader gain spectrum, the stable mode-locked area is continuously extended, while  $V_{\text{SA}}$  higher than  $-2.4$  V is needed to provide sufficient absorption. Under  $-20$  dB OFB strength, the locking region basically remains identical to the free running condition, as indicated by the white solid contour line shown in Fig. 3(b). In addition, the numbers of comb lines are also not influenced by the OFB at this strength, as shown in the colored mapping. As the OFB strength increases to  $-10$  dB in Fig. 3(c), the boundary of the mode-locked region slightly shrinks at a lower injection current from 40 to 106 mA. Further increasing the  $I_{\text{inj}}$ , a river-like unlocked region shows up from  $I_{\text{inj}} = 126$  mA with  $V_{\text{SA}} = -5$  V to  $I_{\text{inj}} = 160$  mA with  $V_{\text{SA}} = -3$  V. At high pump currents, the mode competition becomes stronger due to excessive injected carriers. Moreover, at a high OFB strength, increased intracavity optical energy and back-injected decoherent light enhance the selective gain among different locking modes. As a consequence, the high OFB strength destabilizes the mode-locked laser, ultimately

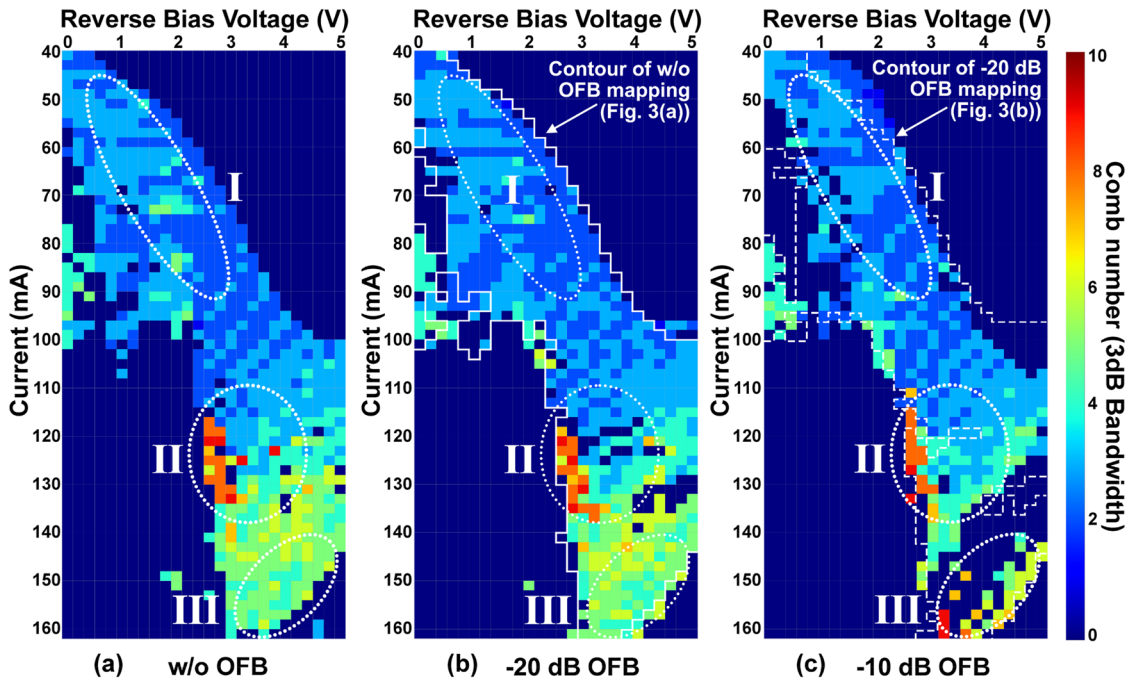


**FIG. 3.** (a) Optical spectrum bandwidth mapping of 100 GHz spaced QD comb laser as a function of SA reverse bias voltage ranging from 0 to  $-5$  V with 0.2 V step and injection current of gain sections varying from 40 to 160 mA with 2 mA step under different OFB strengths: (a) Without OFB, (b)  $-20$  dB OFB and (c)  $-10$  dB OFB. The three different working zones analyzed in detail in the following text have been marked on the graph. The white solid and dashed lines in (b) and (c) represent the stable mode-locking area contour of (a) and (b), respectively.

resulting in an enlarged unlocked region. However, under most of the working conditions, the 100 GHz spaced QD comb laser can still maintain stable locking states under  $-10$  dB OFB strength, which is typically the maximum OFB strength that can be achieved in the optical transmission links.

To further investigate the influence of OFB strength over the QD comb laser, representative working points from three

typical mode-locking zones (circled in Fig. 3) were selected for detailed spectral analysis. Figures 4(a)–4(c) show their spectral evolutions with the OFB strength ranging from  $-45$  to  $-10$  dB. Figures 4(d)–4(f) display the corresponding optical spectra under no OFB,  $-20$ , and  $-10$  dB OFB, respectively. Within zone I region, the envelope of the comb spectrum is roughly Gaussian-shaped. A typical working point ( $I_{\text{inj}} = 58$  mA,  $V_{\text{SA}} = -3$  V) for Gaussian-shaped

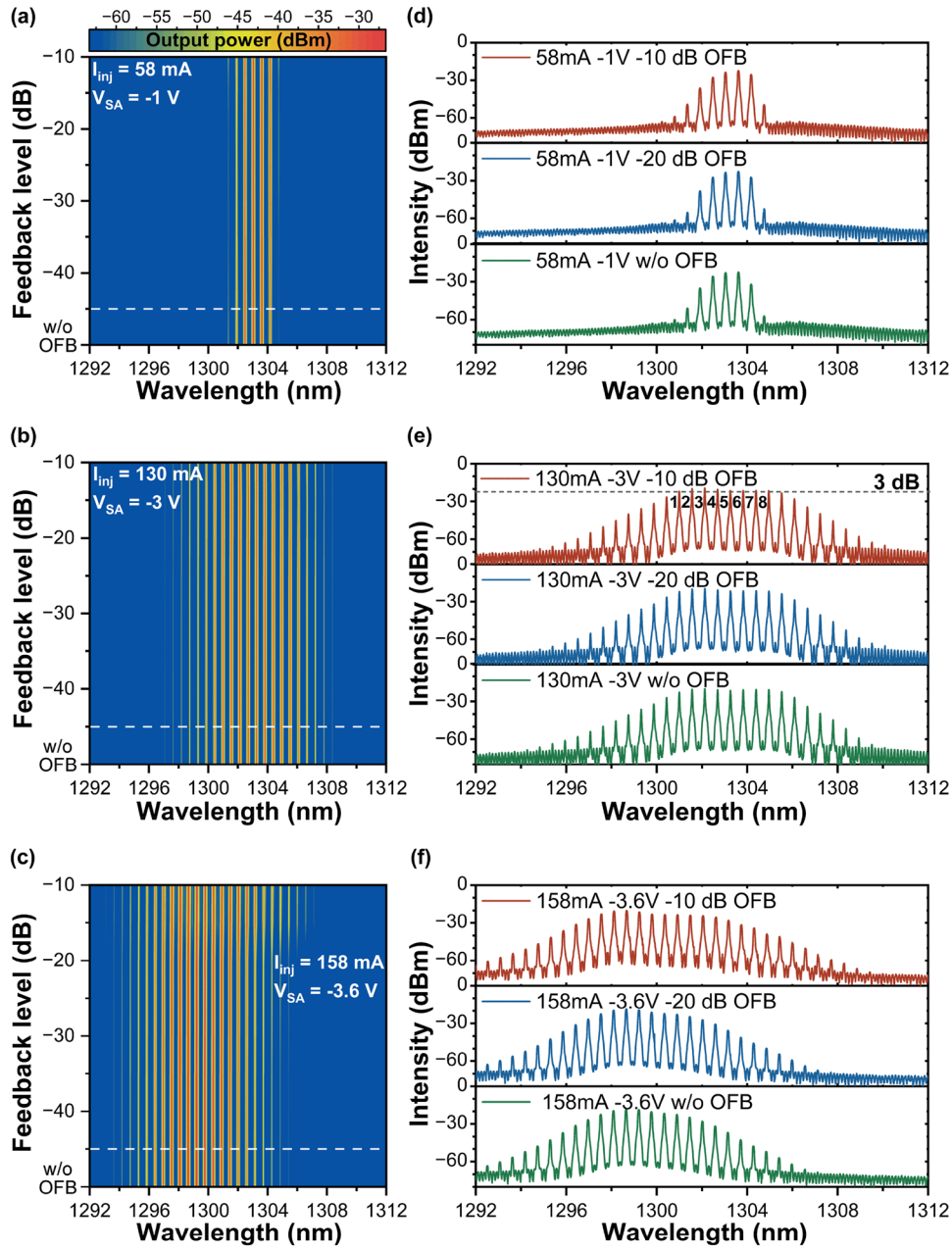


**FIG. 4.** Optical spectral evolution under different OFB strengths of the 100 GHz spaced QD comb laser operating under three typical operation conditions: (a) and (d)  $I_{\text{inj}} = 58$  mA,  $V_{\text{SA}} = -1$  V; (b) and (e)  $I_{\text{inj}} = 130$  mA,  $V_{\text{SA}} = -3$  V; and (c) and (f)  $I_{\text{inj}} = 158$  mA,  $V_{\text{SA}} = -3.6$  V.

comb under OFB is selected for further analysis. The optical spectral evolution in Fig. 4(a) shows that the QD comb laser is highly stable in this locking zone that optical spectra are preserved without wavelength shift at all different OFB strengths. The detailed optical spectra in Fig. 4(d) show that both comb numbers and optical power of each comb remain consistent under varied OFB strengths. A higher injection current brings a broader gain spectrum to form a

flat-top optical frequency comb with improved optical bandwidth,<sup>20</sup> corresponding to zone II in Fig. 3. Similar to the stable Gaussian-shaped comb, both the spectrum evolution and optical spectrum of the comb laser working under a typical flat-top mode-locked condition ( $I_{inj} = 130$  mA,  $V_{SA} = -3$  V) remains feedback-insensitive under all OFB strengths, as shown in Figs. 4(b) and 4(e). Eight comb lines with 100 GHz mode spacing within 3 dB bandwidth of

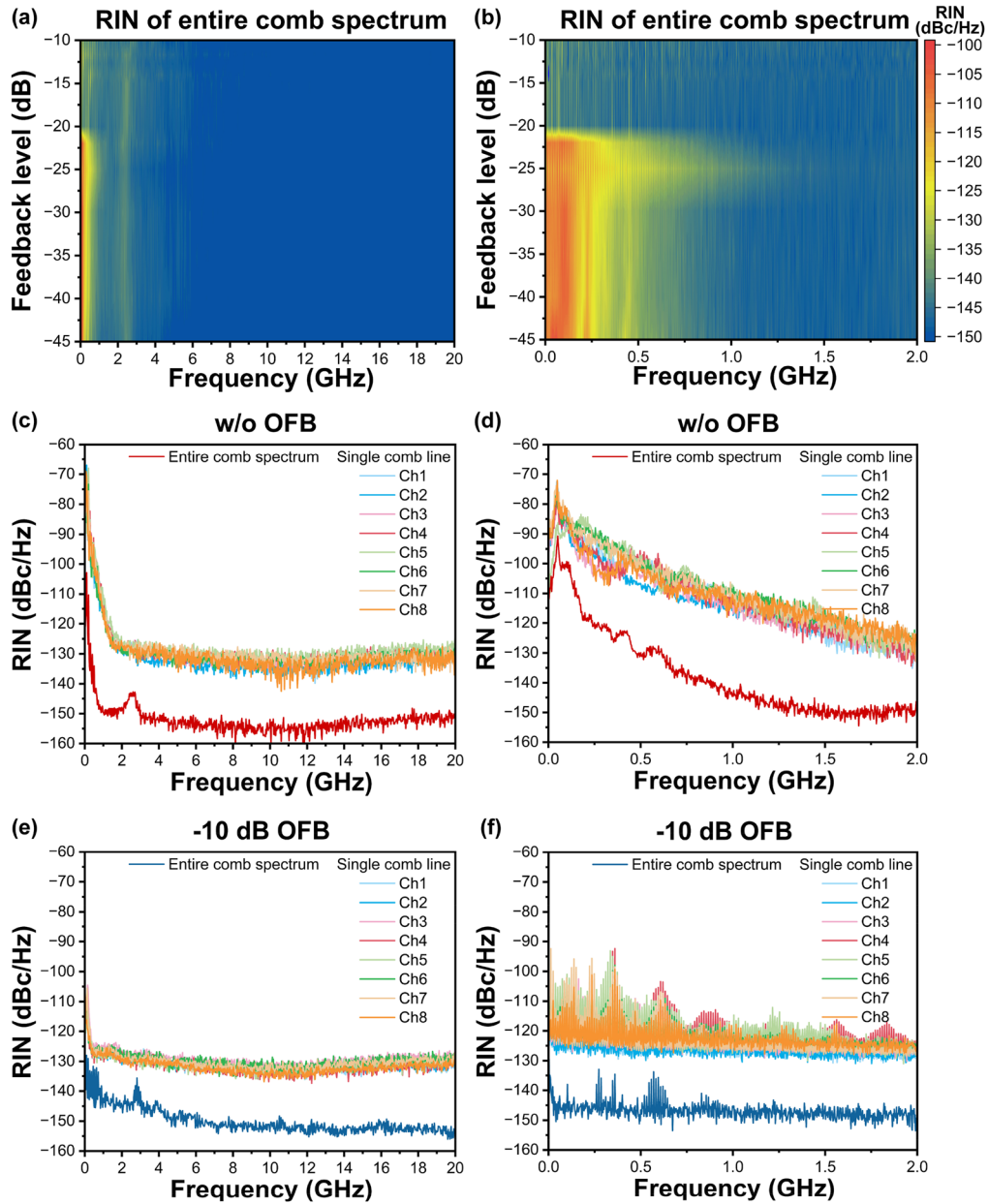


**FIG. 5.** (a) RIN evolution with different OFB strengths of the entire comb spectrum of laser working at  $I_{inj} = 130$  mA and  $V_{SA} = -3$  V. RIN of eight filtered individual comb lines within 3 dB bandwidth and the entire comb spectrum (c) without and (e) under  $-10$  dB OFB, with  $RBW = VBW = 200$  kHz for the ESA. The corresponding RIN within the 0–2 GHz frequency range, measured at  $RBW = VBW = 51$  kHz, is shown in (b), (d), and (f).

745 GHz remain ultra-stable operation in both wavelength and optical power under OFB from  $-45$  to  $-10$  dB. The feedback insensitivity characteristic of the QD comb laser is attributed to the near-zero  $\alpha$  factor measured in the FP QD laser that shares an identical gain structure.<sup>44</sup> Figure 4(c) shows the typical spectral evolution at  $I_{inj} = 158$  mA and  $V_{SA} = -3.6$  V, as a representative of zone III. The wavelength blueshift arises from the quantum confined Stark effect (QCSE), which is pronounced at high  $V_{SA}$ .<sup>15</sup> The spectrum remains unchanged under  $-20$  dB OFB as illustrated in Fig. 4(f). As the OFB strength increases to  $-10$  dB, the overall bandwidth increases, driven by the selective gain enhancement induced by OFB. In addition, as shown in Fig. 4(f), the optical signal–noise ratio (OSNR) of individual comb line decreases from over 40 to 30 dB, suggesting the increased mode competition as well. Overall speaking, in the flat-top mode-locked region (zone II), the laser can provide eight channels with stable wavelength and intensity without the use of

isolators under an OFB strength up to  $-10$  dB. To verify the transmission capability of this QD comb laser, further characterizations of RIN and external modulation experiments are performed at the specific working point ( $I_{inj} = 130$  mA,  $V_{SA} = -3$  V) for subsequent measurements.

For amplitude modulation (AM), the RIN is directly related to the transmission performance, such as eye diagram and BER. Therefore, we characterized the RIN of the entire comb spectrum under different OFB strengths. Figures 5(a) and 5(b) show the RIN evolution of the entire comb spectrum under an OFB strength from  $-45$  to  $-10$  dB across the full frequency range (0–20 GHz) and low-frequency range (0–2 GHz), respectively. At high frequencies, the RIN curves remain at low noise levels and are not influenced by OFB, while at low frequencies without OFB, RIN curves started at high levels around  $-100$  dBc/Hz and gradually

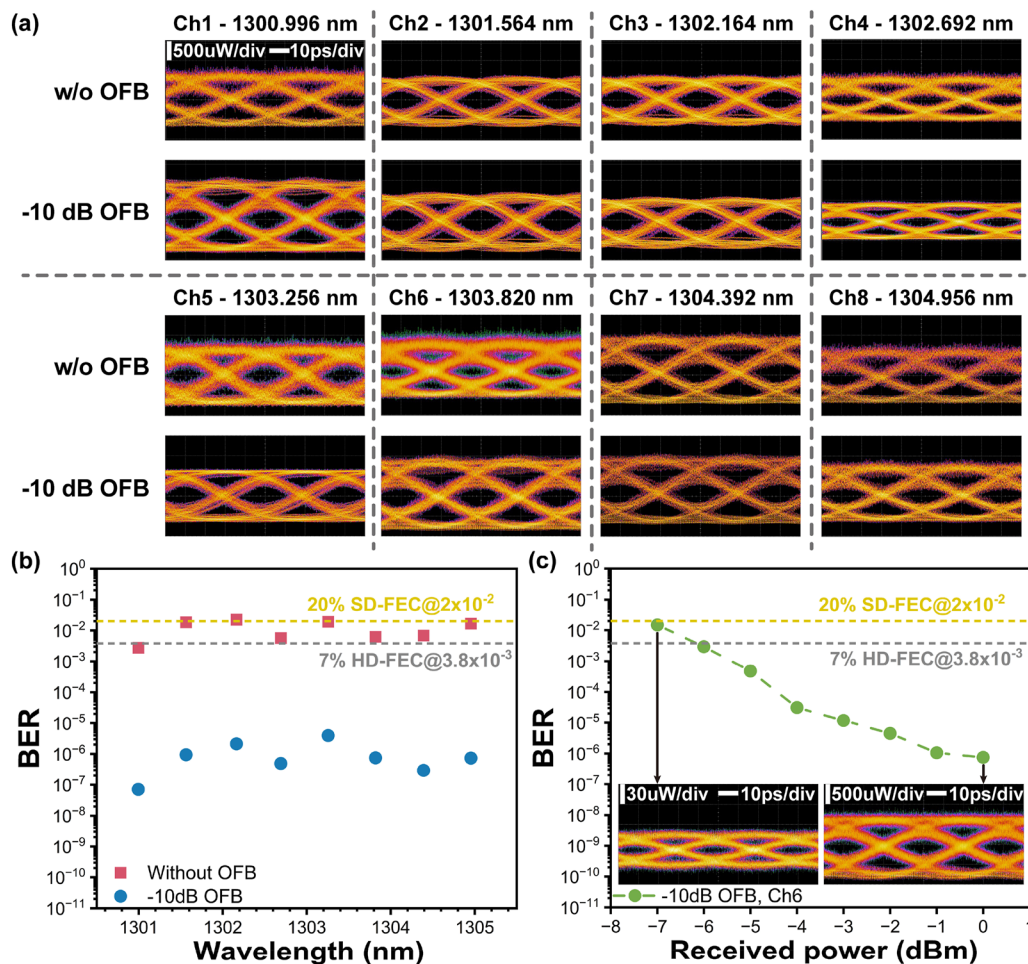


**FIG. 6.** (a) 25 Gbps NRZ optical eye diagrams with a PRBS31 pattern of eight filtered individual comb lines within 3 dB bandwidth. The top row results were measured without OFB, while the corresponding bottom row results were measured under  $-10$  dB OFB. (b) Bite error rate (BER) vs wavelength for 25 Gbps B2B transmission with or without  $-10$  dB OFB. (c) BER vs received optical power for 25 Gbps B2B transmission using the comb line located at 1303.820 nm (channel 6). Insets: Eye diagrams were measured under  $-7$  and  $0$  dBm, respectively.

dropped as frequency increases. The RIN exhibits flat RF spectra without discernible relaxation resonance peaks, confirming that the laser operates in an overdamped regime, which contributes to feedback insensitivity properties.<sup>21</sup> Interestingly, the low-frequency RIN is significantly suppressed when the OFB strength is beyond  $-20$  dB. The low-frequency noise is related to MPN.<sup>45</sup> The MPN is pronounced especially when filtering out a single wavelength from the entire comb spectrum. It indicates jitter within a single comb line, hindering high-order modulation and impairing the transmission system performance.<sup>46,47</sup> As the OFB strength increases, the external OFB enhances the coupling between adjacent modes, which reduces the MPN<sup>48</sup> and RIN. Figures 5(c) and 5(e) compare the RIN spectra of eight filtered comb lines and the entire comb spectrum under free running conditions and  $-10$  dB OFB conditions, respectively. The relatively higher RIN levels of single comb lines are mainly due to the reduced output power in comparison with the whole optical spectrum. Similar to the OFB effects on the whole comb laser spectrum, the high-frequency RIN of each comb line is not affected by the OFB, remaining at  $-130$  dBc/Hz. The RIN reduction phenomenon is also observed for each comb line at the low-frequency range. The peak values of RIN spectra of eight single comb lines are approximately  $-75$  dBc/Hz under free-running conditions [Fig. 5(d)]; by introducing  $-10$  dB OFB, the low-frequency RIN decreases to approximately  $-120$  dBc/Hz [Fig. 5(f)], which indicates 40 dB RIN reduction in the low-frequency range.

To further characterize the transmission performance of QD comb lasers, high-speed external modulation was implemented with a commercial LN MZM. The eye diagram and BER of eight filtered individual comb lines within 3 dB bandwidth are evaluated separately. Figure 6(a) shows the optical eye diagrams for the 25 Gbps NRZ modulation format of eight comb lines for the free running case and under  $-10$  dB OFB. All the eye diagrams exhibit extinction ratios exceeding 3.2 dB. As for the BERs, when there is no OFB, the BERs of all eight combs are below the 20% soft-decision forward error correction (SD-FEC) standard ( $\text{BER} = 2 \times 10^{-2}$ ) as illustrated in Fig. 6(b). However, under  $-10$  dB OFB, the corresponding BER decreased by five orders of magnitude, with a minimum BER of  $7.08 \times 10^{-8}$ . In addition, the BERs of all eight channels are well below the 7% hard-decision forward error correction (HD-FEC) standard ( $\text{BER} = 3.8 \times 10^{-3}$ ). These results are consistent with the significant reduction in low-frequency RIN levels under  $-10$  dB OFB. We selected the sixth comb channel for BER vs received power measurements, and the result under  $-10$  dB OFB is shown in Fig. 6(c). The results indicate that the minimum required optical power for error-free transmission of the current system under  $-10$  dB OFB is approximately  $-7$  dBm. Further reducing the power will lead to a higher BER than the 20% SD-FEC threshold. A high linear photodiode could enhance the receiver's performance in the experimental system and will further reduce the BER, allowing for a lower input power. Taking all the eight comb channels within 3 dB bandwidth into consideration, the GaAs-based InAs/GaAs QD 100 GHz mode-locked laser is capable of 200 Gbps data transmission with the 25 Gbps NRZ modulation format, enhanced by consistent  $-10$  dB OFB. Further optimization of forward error correction (FEC) and digital signal processing (DSP) is expected to enable higher data transmission rates.

#### IV. CONCLUSIONS

We experimentally studied the OFB influence of the InAs/GaAs QD comb laser in various aspects. For static optical properties, the optical spectra of the comb laser can maintain stable locking states with constant comb numbers subjected to the OFB strength up to  $-10$  dB. At a flat-top mode-locked operation point, the low-frequency RIN of the comb laser and individual comb lines show sufficient suppression as OFB level exceeds  $-20$  dB, and their RIN across the entire frequency range reaches  $-130$  dBc/Hz at a high OFB of  $-10$  dB. The high-speed transmission characterization shows great tolerance of the comb laser under a strong OFB. Under  $-10$  dB OFB strength, the eight-filtered comb channels exhibit clear eye-opening with over 3 dB extinction ratio under 25 Gbps NRZ modulation with a PRBS31 pattern. The BER of each channel is further reduced by five orders of magnitude to  $10^{-7}$  range. The feedback-insensitive QD comb laser is capable of supporting 200 Gbps transmission with eight comb lines under OFB up to  $-10$  dB. The overall results indicate that Tbps transmission from a single comb laser is feasible by implementing high-speed modulator arrays (such as thin film LN MZMs or silicon ring modulators). The feedback insensitivity of the QD comb laser makes it a promising isolator-free multi-wavelength light source solution for chip-level, high-density, and high-bandwidth DWDM applications.

#### ACKNOWLEDGMENTS

This research was funded by the National Key Research and Development Program of China (Grant No. 2022YFB2803600), National Natural Science Foundation of China (Grant Nos. 62225407, 12274449, 62334013, and 62005308), and Innovation Program for Quantum Science and Technology (Grant No. 2021ZD0302300). Ting Wang was supported by the Youth Innovation Promotion Association of CAS (Grant No. Y2022005). Zihao Wang was supported by the Youth Innovation Promotion Association of CAS (Grant No. 2023008). Jianan Duan was supported by the Basic and Applied Basic Research Foundation of Guangdong Province (Grant No. 2021A1515110076).

#### AUTHOR DECLARATIONS

##### Conflict of Interest

The authors have no conflicts to disclose.

#### Author Contributions

**Xiangru Cui:** Conceptualization (equal); Data curation (lead); Formal analysis (lead); Investigation (lead); Methodology (equal); Software (equal); Writing – original draft (lead); Writing – review & editing (lead). **Jiajian Chen:** Data curation (supporting); Formal analysis (equal); Writing – original draft (equal). **Jingzhi Huang:** Data curation (supporting); Writing – original draft (supporting). **Bo Yang:** Investigation (supporting); Writing – original draft (supporting). **Jiale Qin:** Software (equal). **Wenlu Wang:** Methodology (supporting); Validation (supporting). **Jianan Duan:** Investigation (supporting); Methodology (supporting); Writing – original draft

(equal). **Ting Wang:** Investigation (supporting); Methodology (supporting); Writing – original draft (equal); Writing – review & editing (equal). **Zihao Wang:** Conceptualization (lead); Funding acquisition (equal); Investigation (supporting); Methodology (equal); Project administration (equal); Supervision (equal); Writing – original draft (equal); Writing – review & editing (lead). **Jianjun Zhang:** Funding acquisition (equal); Project administration (equal); Resources (lead); Supervision (lead); Writing – review & editing (supporting).

## DATA AVAILABILITY

The data that support the findings of this study are available from the corresponding author upon reasonable request.

## REFERENCES

- C. Shang, Y. Wan, J. Selvidge, E. Hughes, R. Herrick, K. Mukherjee, J. Duan, F. Grillot, W. W. Chow, and J. E. Bowers, “Perspectives on advances in quantum dot lasers and integration with Si photonic integrated circuits,” *ACS Photonics* **8**(9), 2555–2566 (2021).
- Y. Lu, X. Hu, M. Tang, V. Cao, J. Yan, D. Wu, J.-S. Park, H. Liu, X. Xiao, and S. Chen, “Analysis of the regimes of feedback effects in quantum dot laser,” *J. Phys. D: Appl. Phys.* **55**(48), 484003 (2022).
- S. Lee, N. Tajima, T. Shindo, D. Takahashi, N. Nishiyama, and S. Arai, “High optical-feedback tolerance of distributed reflector lasers with wirelike active regions for isolator-free operation,” *IEEE Photonics Technol. Lett.* **21**(20), 1529–1531 (2009).
- S. Azouigui, B. Dagens, F. Lelarge, J. G. Provost, A. Accard, F. Grillot, A. Martinez, Q. Zou, and A. Ramdane, “Tolerance to optical feedback of 10-Gb/s quantum-dash-based lasers emitting at 1.51  $\mu\text{m}$ ,” *IEEE Photonics Technol. Lett.* **19**(15), 1181–1183 (2007).
- O. B. Shchekin, G. Park, D. L. Huffaker, Q. Mo, and D. G. Deppe, “Low-threshold continuous-wave two-stack quantum-dot laser with reduced temperature sensitivity,” *IEEE Photonics Technol. Lett.* **12**(9), 1120–1122 (2000).
- G. T. Liu, A. Stintz, H. Li, K. J. Malloy, and L. F. Lester, “Extremely low room-temperature threshold current density diode lasers using InAs dots in  $\text{In}_{0.15}\text{Ga}_{0.85}\text{As}$  quantum well,” *Electron. Lett.* **35**(14), 1163 (1999).
- Y. Arakawa and H. Sakaki, “Multidimensional quantum well laser and temperature dependence of its threshold current,” *Appl. Phys. Lett.* **40**(11), 939–941 (1982).
- D. Bimberg and C. Ribbat, “Quantum dots: Lasers and amplifiers,” *Microelectron. J.* **34**, 323–328 (2003).
- P. Borri, W. Langbein, J. M. Hvam, F. Heinrichsdorff, M.-H. Mao, and D. Bimberg, “Spectral hole-burning and carrier-heating dynamics in InGaAs quantum-dot amplifiers,” *IEEE J. Sel. Top. Quantum Electron.* **6**(3), 544–551 (2000).
- P. Bhattacharya, S. Ghosh, S. Pradhan, J. Singh, Z.-K. Wu, J. Urayama, K. Kim, and T. B. Norris, “Carrier dynamics and high-speed modulation properties of tunnel injection InGaAs-GaAs quantum-dot lasers,” *IEEE J. Quantum Electron.* **39**(8), 952–962 (2003).
- R. Wang, S. F. Yoon, H. X. Zhao, C. Z. Tong, C. Y. Liu, and Q. Cao, “Temperature-dependent study on modal gain and differential gain of 1.3- $\mu\text{m}$  InAs-GaAs QD lasers with different  $p$ -doping levels,” *IEEE Photonics Technol. Lett.* **22**(14), 1045–1047 (2010).
- N. Kirstaedter, O. G. Schmidt, N. N. Ledentsov, D. Bimberg *et al.*, “Gain and differential gain of single layer InAs/GaAs quantum dot injection lasers,” *Appl. Phys. Lett.* **69**(9), 1226–1228 (1996).
- D. Bimberg, N. Kirstaedter, N. N. Ledentsov, Z. I. Alferov, P. S. Kop’ev, and V. M. Ustinov, “InGaAs-GaAs quantum-dot lasers,” *IEEE J. Sel. Top. Quantum Electron.* **3**(2), 196 (1997).
- J. Duan, H. Huang, D. Jung, Z. Zhang, J. Norman, J. E. Bowers, and F. Grillot, “Semiconductor quantum dot lasers epitaxially grown on silicon with low linewidth enhancement factor,” *Appl. Phys. Lett.* **112**(25), 251111 (2018).
- R. Raghunathan, F. Grillot, J. K. Mee, D. Murrell, V. Kovanis, and L. F. Lester, “Tuning the external optical feedback-sensitivity of a passively mode-locked quantum dot laser,” *Appl. Phys. Lett.* **105**(4), 041112 (2014).
- J. S. Cohen and D. Lenstra, “The critical amount of optical feedback, for coherence collapse in semiconductor lasers,” *IEEE J. Quantum Electron.* **27**(1), 10–12 (1991).
- G. Huyet, D. O’Brien, S. P. Hegarty, J. G. McInerney, D. Bimberg, C. Ribbat, V. M. Ustinov, S. S. Mikhlin, A. R. Kovsh, and A. V. Uskov, “Reduced sensitivity to external feedback in quantum dot lasers,” *Proc. SPIE* **5361**, 21 (2004).
- G. Huyet, S. P. Hegarty, D. O’Brien, A. V. Uskov, S. Melnik, O. Carroll, J. G. McInerney, T. Kettler, M. Laemmlin, D. Bimberg, V. M. Ustinov, S. S. Mikhlin *et al.*, “Damping and feedback characteristics of quantum dot semiconductor lasers,” *Proc. SPIE* **5452**, 509 (2004).
- D. Lenstra, T. T. M. Van Schaijk, and K. A. Williams, “Toward a feedback-insensitive semiconductor laser,” *IEEE J. Sel. Top. Quantum Electron.* **25**(6), 1502113 (2019).
- J.-Z. Huang, Z.-T. Ji, J.-J. Chen, W.-Q. Wei, J.-L. Qin, Z.-H. Wang, Z.-Y. Li, T. Wang, X. Xiao, and J.-J. Zhang, “Ultra-broadband flat-top quantum dot comb lasers,” *Photonics Res.* **10**(5), 1308 (2022).
- J. Duan, H. Huang, B. Dong, D. Jung, J. C. Norman, J. E. Bowers, and F. Grillot, “1.3- $\mu\text{m}$  reflection insensitive InAs/GaAs quantum dot lasers directly grown on silicon,” *IEEE Photonics Technol. Lett.* **31**(5), 345–348 (2019).
- M. Kuntz, G. Fiol, M. Lämmlin, D. Bimberg, M. G. Thompson, K. T. Tan, C. Marinelli, A. Wonfor, R. Sellin, R. V. Penty, I. H. White, V. M. Ustinov, A. E. Zhukov, Y. M. Shernyakov, A. R. Kovsh, N. N. Ledentsov, C. Schubert, and V. Marenbert, “Direct modulation and mode locking of 1.3  $\mu\text{m}$  quantum dot lasers,” *New J. Phys.* **6**, 181 (2004).
- M. G. Thompson, K. T. Tan, C. Marinelli, K. A. Williams, R. L. Sellin, R. V. Penty, I. H. White, M. Kuntz, D. Ouyang, I. N. Kaiaender, N. N. Ledentsov, D. Bimberg, V. M. Ustinov, A. E. Zhukov, A. R. Kovsh, F. Visinka, S. Jochum, S. Hansmann, D.-J. Kang, and M. G. Blamire, “Mode locking of InGaAs quantum dot lasers,” *Proc. SPIE* **5452**, 117 (2004).
- M. Laemmlin, G. Fiol, C. Meuer, M. Kuntz, F. Hopfer, A. R. Kovsh, N. N. Ledentsov, and D. Bimberg, “Distortion-free optical amplification of 20–80 GHz modelocked laser pulses at 1.3  $\mu\text{m}$  using quantum dots,” *Electron. Lett.* **42**(12), 697 (2006).
- P. Zhao, A. Liu, and W. Zheng, “80 GHz AlGaInAs/InP colliding-pulse mode-locked laser with high pulse power,” *Appl. Phys. Express* **9**(12), 122701 (2016).
- C.-Y. Lin, F. Grillot, N. A. Naderi, Y. Li, and L. F. Lester, “rf linewidth reduction in a quantum dot passively mode-locked laser subject to external optical feedback,” *Appl. Phys. Lett.* **96**(5), 051118 (2010).
- C. Mesaritakis, C. Simos, H. Simos, A. Kapsalis, I. Krestnikov, and D. Syvridis, “External optical feedback-induced wavelength selection and Q-switching elimination in an InAs/InGaAs passively mode-locked quantum dot laser,” *J. Opt. Soc. Am. B* **29**(5), 1071 (2012).
- M. Haji, L. Hou, A. E. Kelly, J. Akbar, J. H. Marsh, J. M. Arnold, and C. N. Ironside, “High frequency optoelectronic oscillators based on the optical feedback of semiconductor mode-locked laser diodes,” *Opt. Express* **20**(3), 3268 (2012).
- X. Xiao, A. Descos, G. Kurczveil, S. Srinivasan, D. Liang, and R. G. Beausoleil, “Experimental measurement of the tolerance on optical feedback for the heterogeneous silicon quantum dot comb laser,” in *2023 IEEE Silicon Photonics Conference (SiPhotonics)* (IEEE, Washington, DC, 2023), pp. 1–2.
- G. Fiol, M. Kleinert, D. Arsenijević, and D. Bimberg, “1.3  $\mu\text{m}$  range 40 GHz quantum-dot mode-locked laser under external continuous wave light injection or optical feedback,” *Semicond. Sci. Technol.* **26**(1), 014006 (2010).
- D. Arsenijević, M. Kleinert, and D. Bimberg, “Breakthroughs in photonics 2013: Passive mode-locking of quantum-dot lasers,” *IEEE Photonics J.* **6**(2), 0700306 (2014).
- Green Photonics and Electronics*, edited by G. Eisenstein and D. Bimberg (Springer, Cham, 2017).
- C. Kumar and R. Goyal, “Effect of crosstalk in super dense wavelength division multiplexing system using hybrid optical amplifier,” *J. Opt. Commun.* **40**(4), 347–351 (2019).
- M. Sysak, J. Johnson, and D. Lewis, CW-WDM MSA technical specifications rev 1.0, 2021.

- <sup>35</sup>J.-J. Chen, Z.-H. Wang, W.-Q. Wei, T. Wang, and J.-J. Zhang, "Sole excited-state InAs quantum dot laser on silicon with strong feedback resistance," *Front. Mater.* **8**, 648049 (2021).
- <sup>36</sup>A. He, Y. Cui, J. Xiang, W. Wei, Z. Wang, T. Wang, X. Guo, and Y. Su, "Ultra-low loss SiN edge coupler for III-V/SiN hybrid integration," *Laser Photonics Rev.* **17**(10), 2300100 (2023).
- <sup>37</sup>J.-Z. Huang, W.-Q. Wei, J.-J. Chen, Z.-H. Wang, T. Wang, and J.-J. Zhang, "P-doped 1300 nm InAs/GaAs quantum dot lasers directly grown on an SOI substrate," *Opt. Lett.* **46**(21), 5525 (2021).
- <sup>38</sup>D. Bimberg, M. Grundmann, F. Heinrichsdorff, N. N. Ledentsov, V. M. Ustinov, A. E. Zhukov, A. R. Kovsh, M. V. Maximov, Y. M. Shernyakov, B. V. Volovik, A. F. Tsatsul'nikov, P. S. Kop'ev, and Z. I. Alferov, "Quantum dot lasers: Breakthrough in optoelectronics," *Thin Solid Films* **367**, 235 (2000).
- <sup>39</sup>S. Liu, X. Wu, D. Jung, J. C. Norman, M. J. Kennedy, H. K. Tsang, A. C. Gossard, and J. E. Bowers, "High-channel-count 20 GHz passively mode-locked quantum dot laser directly grown on Si with 41 Tbit/s transmission capacity," *Optica* **6**(2), 128 (2019).
- <sup>40</sup>S. Liu, T. Komljenovic, S. Srinivasan, E. Norberg, G. Fish, and J. E. Bowers, "Characterization of a fully integrated heterogeneous silicon/III-V colliding pulse mode-locked laser with on-chip feedback," *Opt. Express* **26**(8), 9714 (2018).
- <sup>41</sup>X. Huang, A. Stintz, H. Li, L. F. Lester, J. Cheng, and K. J. Malloy, "Passive mode-locking in 1.3  $\mu\text{m}$  two-section InAs quantum dot lasers," *Appl. Phys. Lett.* **78**(19), 2825–2827 (2001).
- <sup>42</sup>S. Liu, J. C. Norman, D. Jung, M. Kennedy, A. C. Gossard, and J. E. Bowers, "Monolithic 9 GHz passively mode locked quantum dot lasers directly grown on on-axis (001) Si," *Appl. Phys. Lett.* **113**(4), 041108 (2018).
- <sup>43</sup>L. A. Coldren, S. W. Corzine, and M. L. Mašanović, *Diode Lasers and Photonic Integrated Circuits*, 1st ed. (Wiley, 2012).
- <sup>44</sup>W. Wang, Z. Wang, T. Wang, J. Chen, J. Zhang, J. Wang, X. Xu, Y. Yao, and J. Duan, "Reflection and temperature insensitive quantum dot lasers," *Proc. SPIE* **12311**, 123110D (2022).
- <sup>45</sup>Q. T. Nguyen, P. Besnard, L. Bramerie, A. Shen, A. Garreau, O. Vaudel, C. Kazmierski, G.-H. Duan, and J.-C. Simon, "Using optical injection of Fabry-Perot lasers for high-speed access in optical telecommunications," *Proc. SPIE* **7720**, 77202D (2010).
- <sup>46</sup>K. Ogawa, "Chapter 8 semiconductor laser noise: Mode partition noise," *Semicond. Semimetals* **22**, 299–330 (1985).
- <sup>47</sup>K. Ogawa, "Analysis of mode partition noise in laser transmission systems," *IEEE J. Quantum Electron.* **18**(5), 849–855 (1982).
- <sup>48</sup>Y. K. Chen, M. C. Wu, T. Tanbun-Ek, R. A. Logan, and M. A. Chin, "Multicolor single-wavelength sources generated by a monolithic colliding pulse mode-locked quantum well laser," *IEEE Photonics Technol. Lett.* **3**(11), 971–973 (1991).